SSRG International Journal of Electrical and Electronics Engineering
ISSN: 2348-8379/ https://doi.org/10.14445/23488379/IJEEE-V10I9P117

Volume 10 Issue 9, 181-189, September 2023

Original Article

Optimal Location of Electric Vehicle Fast Charging Station Using Grasshopper Optimization Algorithm

Zuhaila Mat Yasin[1*], Nur Ashida Salim[2], Siti Zaliha Mohamad Noor[1], Nur Fadilah Ab Aziz[3], Hasmaini Mohamad[2]

[1]*Solar Research Institute (SRI), Universiti Teknologi MARA, Shah Alam, Malaysia.*
[2]*School of Electrical Engineering, College of Engineering, Universiti Teknologi MARA, Shah Alam, Malaysia.*
[3]*School of Electrical Engineering, College of Engineering, Universiti Tenaga Nasional, Malaysia.*

[*]*Corresponding Author : zuhai730@uitm.edu.my*

Received: 23 July 2023 Revised: 26 August 2023 Accepted: 18 September 2023 Published: 30 September 2023

Abstract - *The increasing prevalence of Electric Vehicles (EVs) has underscored the critical importance of establishing a comprehensive and effective charging station network. To sufficiently meet the energy demands of electric vehicles, it is imperative to establish a robust charging station infrastructure that can effectively cater to a substantial volume of electric automobiles. This infrastructure must be widely deployed to ensure widespread accessibility and usability. Many EVs' concurrent usage of electric charging stations may lead to potential unreliability in the distribution setup. Hence, it is imperative to strategically determine the placement and sizing of Fast Charging Stations (FCS) to achieve optimal functionality of the power grid. This paper proposes the Grasshopper Optimization Algorithm (GOA) as a technique for strategically locating FCS to minimize costs. GOA is a computational technique that addresses optimization challenges by formulating a mathematical model that emulates the collective behaviour observed in natural grasshopper swarms. The proposed methodology is evaluated on an IEEE 69-bus radial distribution system. The results indicate that the proposed methodology has successfully identified the most economically efficient location for FCS within a power distribution network compared to alternative optimization methods.*

Keywords - *Ant colony optimizer, Cost minimization, Distribution system, Minimum voltage, Power loss minimization.*

1. Introduction

Internal combustion vehicles have the downside of causing a harmful environmental impact while eventually becoming less effective and using fuel supplies that are getting more costly. The mid-2000s energy crisis sparked increased industrial Electric Vehicle (EV) research and growth due to significant fears over rapidly rising oil prices and the global warming crisis [1-3]. An electric motor powered by electricity stored in batteries or other energy storage systems powers an EV [4-5].

Electric cars need charging facilities, which may be located at home or in public areas. Electric vehicle charging stations, part of an electricity grid that delivers electricity to the future global population of electric cars, are commonly referred to as EV charging stations. The demand for an efficient charging station infrastructure has grown as the number of EVs has increased. According to the Global EV Outlook for 2020, in the first four months of 2020, the four main European vehicle markets (France, Germany, Italy, and the United Kingdom) recorded sales of over 145,000 electric vehicles, which was a 90% increase over the same period in the previous year. Between January and April 2020, the number of electric cars sold in Norway, the nation with the most significant percentage of electric vehicles in overall auto sales, was almost the same as in the same period in 2019 despite the COVID-19 pandemic [6].

The advancement of EVs has also widened the options of charging types used by the electric transportation system [7]. As the charging process is critical to the success of the electric vehicle, most automotive manufacturers across the globe have devoted significant financial resources to the study of charging models [8].

The proper installation of charging station infrastructure is required to offer sufficient energy storage for electric cars, and these stations must be widely built to handle large numbers of electric vehicles. The distribution system may become unreliable when several EVs utilize electric charging stations at the same time. Losses in distribution grids should be kept to a minimum, while the voltage at buses and the actual load remain within acceptable limits to reduce cost and increase efficiency [9-10]. There exist four distinct charging models for Electric Vehicles (EVs) that can be discerned:

- Charging using constant current and constrained voltage: In an in-series battery configuration, the charging process involving constant current and limited voltage is commonly employed. Regrettably, due to the nonlinearity of the charging process, batteries charged in this manner have a diminished longevity. Another limitation, when compared to alternative devices, is the relatively low overall charging rate [11].
- Constant voltage and restricted current charging: The method of constant voltage and regulated current charging has the notable benefit of a considerably reduced charging time in comparison to the initial model. However, it is essential to acknowledge that this particular model's utilization leads to a notably elevated starting current, posing a risk of damaging the electrical equipment in the battery infrastructure [12].
- DC Fast Charging battery: The DC Fast Charging battery utilizes a periodic current pulse and a significant negative current pulse. One notable benefit is the increased charging speed, which comes at the expense of reduced battery life [13]. Figure 1 depicts a standard DC Fast Charging Station [14], whereas Figure 2 presents the basic circuit diagram of a DC Fast Charging system [15].
- Three-stage charging: The three-stage charging approach divides charging into two distinct phases. In the initial stage, a consistent flow of electric current is employed to facilitate the battery's charging process until it reaches its designated terminal voltage. During the second phase, the electrical current gradually reduces in magnitude when a constant voltage is applied [16]. This paradigm can be conceptualized as an intermediary between the initial and subsequent categories.

Several studies have been conducted to determine the most effective placement of fast charging stations through optimization methodologies. The research conducted in [17] utilized the Ant Colony Optimization (ACO) algorithm to ascertain the optimal location of a DC fast charging station within the power grid infrastructure.

This investigation considered the traffic limitations imposed by the residential power grid and prioritized the security of the power system. The ACO algorithm was discovered to determine the ideal placement of a rapid charging station efficiently, hence facilitating the daily recharging of all vehicles' batteries. The efficacy of the ACO algorithm in addressing this problem is evidenced by the high solution quality, as indicated by the low value of the standard deviation.

In addition, a scholarly investigation on the identification of optimal locations for Electric Vehicle (EV) charging stations was documented in [18], employing the Adaptive Particle Swarm Optimization (APSO) algorithm.

This methodology was implemented to decrease the overall cost of charging stations by incorporating traffic flow as a limiting factor. The study focused on examining a district in Beijing, including 103.08 square kilometres, utilizing the upgraded PSO technique.

The conventional PSO technique exhibits a rapid convergence rate. Nevertheless, it is accompanied by significant limitations, including restricted accuracy and susceptibility to divergence. It utilized the inertia factor technique to mitigate the departure of the standard PSO algorithm. This technique involves continuously adjusting the magnitude of the inertial factor throughout the computation phase.

In a previous study [19], the problem of determining the ideal position and size of EV Charging Stations was addressed. This problem was formulated as a Mixed-Integer Non-Linear (MINLP) problem and solved using a Genetic Algorithm (GA). The authors employed the proposed strategy to mitigate the overall expenses, encompassing the costs associated with establishing stations and electrification and the expenditures incurred owing to EV and energy losses in the electric grid resulting from EV charging.

In addition to examining roadways in metropolitan areas, the study incorporated an analysis of potential station placements and the computation of energy losses for EVs. The proposed methodology has been investigated regarding its utilization in examining the impact of different policies on the development of stations. This study aimed to evaluate the effect of power grid reliability on the placement and sizing of charging stations, explicitly focusing on assessing charging cost loss by utilizing a proposed index.

Fig. 1 Example of DC fast charging station

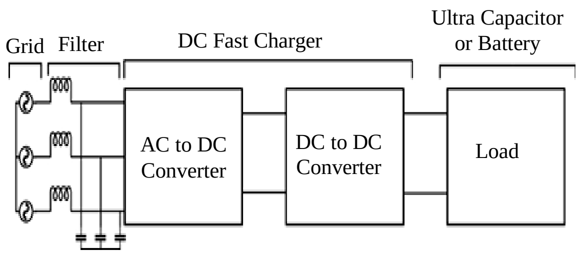

Fig. 2 General circuit of DC fast charging

Each strategy proposed in earlier studies possesses its own set of positive aspects and disadvantages as well. In engineering, the process of identifying and achieving optimal solutions is frequently marked by considerable complexity. This complexity mainly arises from the intricate and non-linear structure of the problems being studied. A notable duration and considerable computational time distinguish the technique. Hence, employing an efficient optimizer to compute optimal solutions is imperative.

Recently, the use of the Grasshopper Optimization Algorithm (GOA) has been prevalent across various domains, showcasing impressive outcomes. The inspiration for GOA stems from observing and emulating grasshoppers' swarming activity in their natural environment, hence categorizing it as a swarm intelligence (SI) technique [20]. The GOA algorithm can generate optimal solutions for many engineering issues. However, more enhancement is required to effectively address the challenges posed by these problems [21-23].

Hence, this research study presents the utilization of GOA to determine the most advantageous placement of fast charging stations to minimize the total cost. The study also compares the total cost and power loss results obtained in this research with those achieved using Ant Colony Optimization (ACO).

2. Materials and Methods

This paper uses GOA to determine the optimum sites for EV fast charging stations in a power grid. The approach is used on a system with a pre-existing grid topology and load data derived from known measurements. The formulation of the objective function and the constraints considered are explained in subsections 2.1 and 2.2, respectively.

2.1. Objective Function

The objective function considered is minimizing the total cost of FCS installation, including initial investment, annual operating, yearly travel, and energy loss costs. An initial investment in a charging station *(C_{INV})* can be calculated using Equation 1 where n is the number of new charging stations, F_{CS} is the investment cost of the charging station, *h, k* is the investment return rate, namely the discount rate, and *m* is the return-on-investment period.

$$C_{INV} = \sum_{h=1}^{nFCS} F \left[\frac{k(1+k)^m}{(1+k)^m - 1}\right] \quad (1)$$

The annual operating cost for the charging station (C_{OM}) can be calculated using Equation 2, where C_{OM} includes maintenance costs, cost of materials, employee wages, and cost of electricity. It may be transformed to become the initial investment costs, where α is a conversion coefficient.

$$C_{OM} = \sum_{h=1}^{nFSH} \alpha F \quad (2)$$

The yearly travel costs of all EVs to charge at the FCS (C_{TRV}) are calculated based on Equation 3, where wear and tear cost considers the expense of driving an EV to a fast-charging station to replenish the battery over the span of a year [20]. In Equation 3, *t* is the road twist coefficient, *η* the smooth traffic coefficient, *L* is the loss coefficient, *n* is the number of charging stations, *c* is the annual charging times per vehicle, and *z* is the turnaround coefficient. When '*hp*' is the collection of vehicles travelling to charging station h for charging at point p, Ghp denotes the criteria determining whether a car at point *p* moves to set station *h* for charging. *Dhp* indicates the distance between charging station h and the vehicle at point *p*.

$$C_{TRV} = \eta tcz \ \sum_{h=1}^{n} \sum_{p \, \epsilon \, hp} G_{hp} \, L \, D_{hp} \quad (3)$$

Equation 4 outlines the mathematical expression that represents the annual cost of energy loss on a power line with an FCS installed in a residential power distribution grid, denoted as C_{EL}. In this equation, the variable "*e*" represents the unit price of electricity per kilowatt-hour in the power distribution grid. "Ploss" refers to quantifying power loss in a distribution system line. Equation 5 can express the factual power dissipation in a power distribution system line, where *I* represent the electric current, and *Ri* represents the resistance of line *i*. The acronym *NB* means the number of branches inside the electric distribution system.

$$C_{EL} = 365 \ \times e \times o \times P_{loss} \quad (4)$$

$$P_{loss} = \sum_{i=1}^{NB} |I|^2 \, R_i \quad (5)$$

The system is constructed to minimize the C_{TOTAL} of C_{INV}, C_{OM}, C_{TRV}, and C_{EL}, as shown in Equation 6, where C_{TOTAL} denotes the total cost of annual investment expenses, running costs, EV travel costs, and costs caused by power losses in power distribution lines after FCS installation.

$$C_{TOTAL\,(min)} = \text{Min}\,[C_{INV} + C_{OM} + C_{TRV} + C_{EL}] \quad (6)$$

2.2. Constraint

Constraints of the fast-charging station's installed location are shown in equation (7) where *lf(h)* is the charging station *h*'s load factor, *chg_cap* is the charging station *h*'s capacity and $cos\ \theta_h$ is the charging station *h'*s power factor.

P_h is the total load of all cars charging at station h daily; R_h denotes the charging radius of charging station h and is a traffic constraint of FCS for EVs; and Equation 7 denotes that each vehicle charges at only one station.

$$\sum_{h=1}^{n} G_{hp} = 1 \tag{7}$$

$$D_{ph} \leq R_h \tag{8}$$

$$P_h < \frac{\text{chg\_cap}_h \text{ x lf(h) x } \cos\theta_h \text{ x o}}{\text{chg\_time x lfv}},\ h = 1,2,..,n \tag{9}$$

The security requirements of the power distribution system encompass limitations on the voltage magnitude of all buses, as well as the scattered loadings on the lines, as depicted in Equation 8. Equation 9 presents the line loading (Si) for each line within the distribution grid. Here, N_B represents the total number of buses within the distribution system, while N_S indicates the total number of sections present within the distribution system.

$$V_i^{min} \leq V_i \leq V_i^{max}, i \in N_B \tag{10}$$

$$S_i \leq S_i^{max}, i \in N_S \tag{11}$$

2.3. Test System and EV Parameters

An individual EV fast charging station has a capacity of 500 kVA. To validate the results of the GOA, an IEEE 69 radial bus test system is categorized into six zones, as shown in Figure 3. Table 1 and 2 exhibit system data of the test system and the buses categorized in each zone, respectively. Table 3 summarizes the parameters of an EV charging station. For 69 buses, the base MVA is 100 MVA, and the base voltage is 22 kV.

Table 1. System data of modified IEEE 69-bus test system

From Bus	To Bus	R (p.u)	X (p.u)	Bus No.	Pload (MW)	Qload (MVAR)	From Bus	To Bus	R (p.u)	X (p.u)	Bus No.	Pload (MW)	Qload (MVAR)
1	2	0.0003	0.0007	1	0	0	36	37	0.0399	0.0976	36	0.026	0.01855
2	3	0.0003	0.0007	2	0	0	37	38	0.0657	0.0767	37	0.026	0.01855
3	4	0.0009	0.0022	3	0	0	38	39	0.0190	0.0221	38	0	0
4	5	0.0157	0.0183	4	0	0	39	40	0.0011	0.0013	39	0.024	0.017
5	6	0.2283	0.1163	5	0	0	40	41	0.4543	0.5308	40	0.024	0.017
6	7	0.2377	0.1211	6	0.0026	0.0022	41	42	0.1934	0.2260	41	0.0012	0.001
7	8	0.0575	0.0293	7	0.0404	0.03	42	43	0.0256	0.0298	42	0	0
8	9	0.0308	0.0157	8	0.075	0.054	43	44	0.0057	0.0072	43	0.006	0.0043
9	10	0.5109	0.1689	9	0.03	0.022	44	45	0.0679	0.0857	44	0	0
10	11	0.1168	0.0386	10	0.028	0.019	45	46	0.0006	0.0007	45	0.0392	0.0263
11	12	0.4438	0.1467	11	0.145	0.104	4	47	0.0021	0.0052	46	0.0392	0.0263
12	13	0.6425	0.2121	12	0.145	0.104	47	48	0.0531	0.1299	47	0	0
13	14	0.6513	0.2152	13	0.008	0.0055	48	49	0.1808	0.4424	48	0.079	0.0564
14	15	0.66	0.2181	14	0.008	0.0055	49	50	0.0513	0.1255	49	0.3847	0.2745
15	16	0.1226	0.0405	15	0	0	8	51	0.0579	0.0295	50	0.3847	0.2745
16	17	0.2336	0.0772	16	0.0455	0.03	51	52	0.2070	0.0695	51	0.0405	0.0283
17	18	0.0029	0.0010	17	0.06	0.035	9	53	0.1085	0.0553	52	0.0036	0.0027
18	19	0.2044	0.0676	18	0.06	0.035	53	54	0.1266	0.0645	53	0.0043	0.0035
19	20	0.1314	0.0434	19	0	0	54	55	0.1733	0.0903	54	0.0264	0.019
20	21	0.2131	0.0704	20	0.001	0.0006	55	56	0.1755	0.0894	55	0.024	0.0172
21	22	0.0087	0.0029	21	0.114	0.081	56	57	0.9919	0.3329	56	0	0
22	23	0.0993	0.0328	22	0.0053	0.0035	57	58	0.4889	0.1641	57	0	0
23	24	0.2160	0.0714	23	0	0	58	59	0.1898	0.0628	58	0	0
24	25	0.4671	0.1544	24	0.028	0.02	59	60	0.2409	0.0731	59	0.1	0.072
25	26	0.1927	0.0637	25	0	0	60	61	0.3166	0.1613	60	0	0
26	27	0.1080	0.0357	26	0.014	0.01	61	62	0.0608	0.0309	61	1.244	0.888
3	28	0.0027	0.0067	27	0.014	0.01	62	63	0.0905	0.0460	62	0.032	0.023
28	29	0.0399	0.0976	28	0.026	0.0186	63	64	0.4432	0.2258	63	0	0
29	30	0.2482	0.0820	29	0.026	0.0186	64	65	0.6494	0.3308	64	0.227	0.162
30	31	0.0438	0.0145	30	0	0	11	66	0.1255	0.0381	65	0.059	0.042
31	32	0.2190	0.0724	31	0	0	66	67	0.0029	0.0009	66	0.018	0.013
32	33	0.5234	0.1757	32	0	0	12	68	0.4613	0.1525	67	0.018	0.013
33	34	1.0655	0.3522	33	0.014	0.01	68	69	0.0029	0.0010	68	0.028	0.02
34	35	0.9195	0.3040	34	0.0195	0.014					69	0.028	0.02
3	36	0.0027	0.0067	35	0.006	0.004							

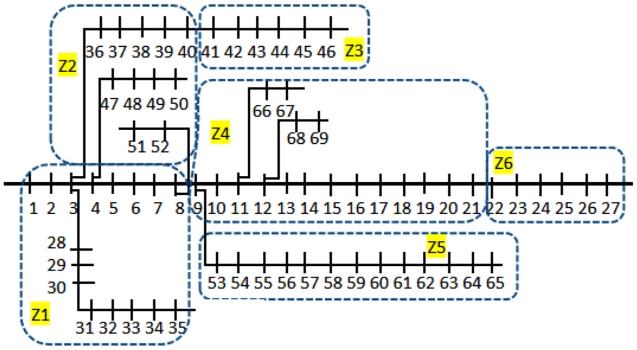

Fig. 3 Single line diagram of IEEE 69-bus distribution test system

Table 2. Buses in each zone

Zone	Buses
1	1,2,3,4,5,6,7,8,28,29,30,31,32,33,34,35
2	36,37,38,39,40,47,48,49,50,51,52
3	41,42,43,44,45,46
4	9,10,11,12,13,14,15,16,17,18,19,20,21,66,67,68, 69
5	53,54,55,56,57,58,59,60,61,62,63,64,65
6	22,23,24,25,26,27

Table 3. Parameters of EV charging station [17]

Specification	Parameter
EV FST load factor (lf)	0.95
Load factor of EV (lfv)	0.5
The service time of EV FST (o)	24 hours
Charging time of each EV (chg_time)	0.25 hours
Charging station capacity (chg_cap)	500 kVA
Power factor	1
Road twist coefficient (t)	1.1
Turnaround coefficient (z)	1.5
Smooth traffic coefficient (η)	1.1
Loss coefficient (L)	1.3
Annual charging times per vehicle (c)	180
Simultaneity factor (f1)	0.95
Demand factor (f2)	0.95
Charging efficiency (q)	0.9
Charging radius (R)	1.2 km
Capital recovery period (m)	20 years
Discount rate (k)	0.1
Conversion coefficient (α)	1.2
Initial investment (F)	10,000,000 Yuan

2.4. Grasshopper Optimization Algorithm (GOA)

To tackle optimization issues, the Grasshopper Optimization Algorithm (GOA) theoretically recreates and replicates the swarming behaviour of grasshoppers in their natural environment. Two opposing forces exist between grasshoppers: repulsion and attraction forces. Attraction forces urge grasshoppers to exploit potential locations (local search), while repulsion forces drive them to explore the search space (global search). The location where the stated details cancel each other out or are the same is referred to as the comfort zone, as shown in Figure 4. The grasshoppers' location has the highest fitness when the target location is undiscovered, as it is the closest to the target [20]. To achieve the objective, grasshoppers keep moving in the same direction as the target in their social interaction network. The locations of grasshoppers are updated to maintain an equilibrium between global and local search; therefore, the comfort zone will adjust to disappear. Grasshoppers eventually reach a point of convergence and discover the optimal solution after following the exploitation and exploration procedure [21].

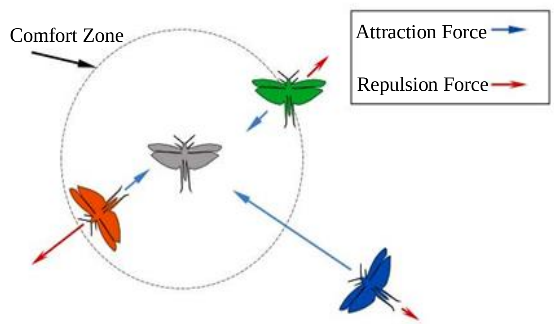

Fig. 4 Social interaction of grasshoppers

Figure 5 is a flowchart illustrating a GOA utilized to determine the most optimal deployment strategy for EV fast charging stations. To begin with, the initial values of the declining coefficient parameter (*Cmax*), minimum (*Cmin*) values, the parameters of appealing length scale (*l*), the strength of the attraction (*f*), the maximum number of iterations (*maxitr*), and the initial iteration (*t*) are initialized. To prevent premature convergence, which can result in the fitness function becoming caught in local minima, it is crucial to determine the swarm's size appropriately. This ensures a balance between achieving accurate convergence and minimizing computational time. According to [24], an enormous swarm size will increase calculation time. The number of grasshoppers, maximum iterations, and variables set in the GOA are 20, 100, and 6, respectively.

Subsequently, the initial population is generated by a random process, adhering to the predetermined constraints. The value of each solution is determined by evaluating the objective function. The primary focus of this study pertains to minimizing costs, as shown in the objective function.

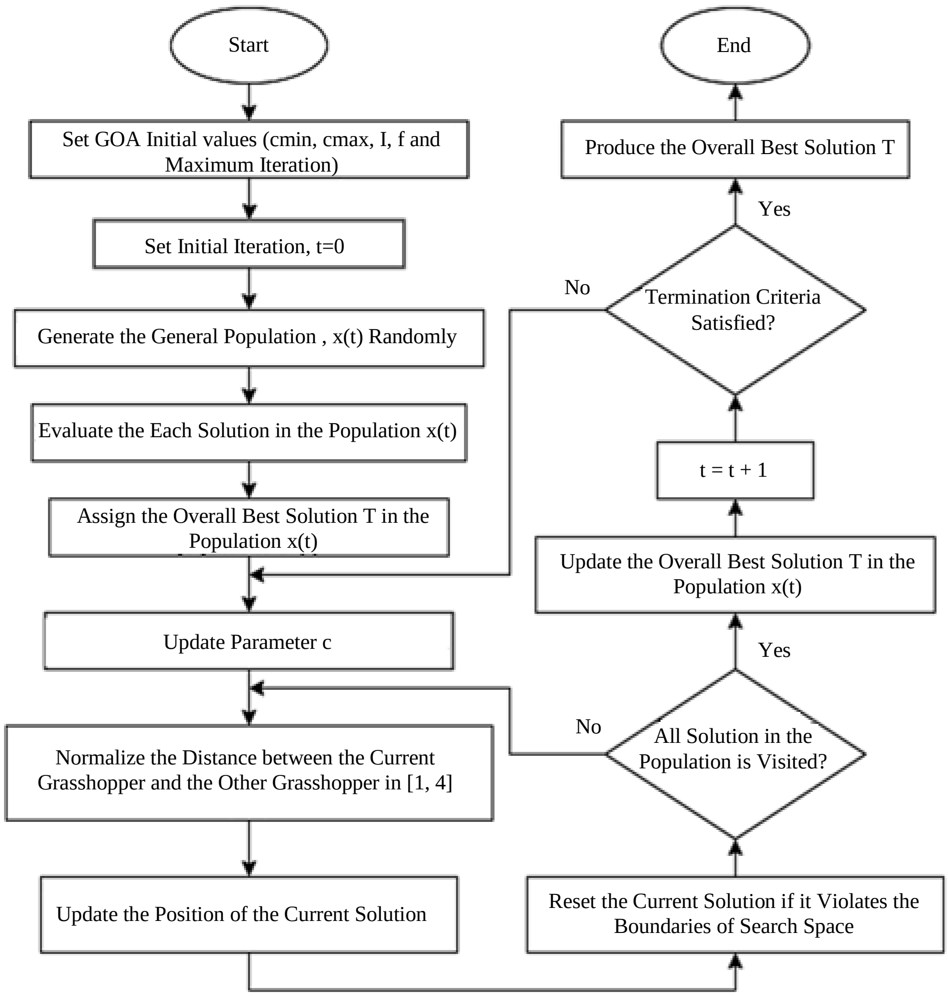

Fig. 5 Flowchart of GOA for optimal BESS planning

The optimal answer, the global best solution, is determined by evaluating all potential solutions within the initial population and assigning the key with the highest value. The coefficient parameter *c* gets updates using Equation 12 during each iteration to diminish the comfort, repulsion, and attraction zones [18]. In the present stage, "*l*" represents the current iteration, while "*L*" denotes the maximum number of iterations.

$$C = Cmax - l\,\frac{Cmax - Cmin}{L} \qquad (12)$$

The variable *s* in Equation 13 is utilized to partition the search space into distinct regions characterized by comfort, repulsion, and attraction. Additionally, *s* is the function that quantifies the two social forces' relative strengths, attraction and repulsion, acting between the grasshoppers. The manipulation of parameters *f* and *l* has the potential to exert an influence on social behaviour.

$$s(r) = f e^{\frac{-r}{l}} - e^{-r} \qquad (13)$$

When the distance between two grasshoppers exceeds ten units, their capacity to partition the stated search space diminishes to zero. Therefore, to address this matter, the spatial separation between the grasshoppers is graphically represented on the interval [1,4]. Equation 14 delineates that the global best solution of the population is adjusted by considering its proximity to the other solutions, the coefficient parameter c, and the distance between it and the other answers. In the given equation, the variables "*ubd*" and "*lbd*" represent the upper and lower bounds in the dth dimension. The goal value in the d^{th} dimension is denoted as $\hat{T}d$ [20].

$$X_i = \mathrm{c} \sum_{j=1}^{N} c \left(\frac{ubd - lbd}{2}\, s\left(\left|X_j^d - X_i^d\right|\right) \frac{Xj - Xi}{dij} \right) + \hat{T}\mathrm{d} \qquad (14)$$

If the revised solution surpasses its prescribed upper or lower limits, it reverts to its original domain. Subsequently, the three processes mentioned above are repeated iteratively for every solution inside the population. Therefore, the solutions proposed by the population are regularly updated and evaluated, and ultimately, the most optimal global solution is selected. The overall operations are iterated until the maximum number of repetitions (*maxitr*) is achieved; at this point, the task terminates. When the algorithm reaches its maximum number of iterations, it returns the optimal global solution *T* [20].

3. Results and Discussion

The simulation results from the Genetic Optimization Algorithm (GOA) and the Ant Colony Optimization (ACO) are summarized in Table 4. A slight discrepancy exists between the rankings of the most optimal Fast Charging Stations (FCS) as assessed by the GOA and ACO. When implementing the GOA technique, the overall cost of FCS is projected to be 80,788,069 Yuan, in contrast to the cost of 85,795,700 Yuan associated with using the ACO approach.

Table 4. Results of GOA and ACO

Stations	GOA	ACO
FCS 1	28	6
FCS 2	39	37
FCS 3	44	43
FCS 4	9	69
FCS 5	53	61
FCS 6	23	23
Total Cost	80,788,069 Yuan	85,795,700 Yuan
Power Loss	0.3344 kW	0.3469 kW

The results indicate that, compared to ACO, GOA demonstrates the ability to locate optimal locations that provide the lowest fitness level. The dispersion of the FCS can be observed across the power distribution system of each zone. Regions characterized by high-density residential dwellings surround each FCS site.

The power system performance, specifically power loss and voltage profile, is influenced by the power consumption of FCS. Nevertheless, the utilization of GOA leads to reduced power losses and an enhanced voltage profile compared to ACO. The minimum voltage and total power losses observed utilizing the Grid Optimization Algorithm (GOA) are 0.8986 per unit (p.u.) and 0.3344 kilowatts (kW), respectively.

The behaviour of the GOA to the parameter space and the search history during the optimization process is depicted in Figure 6. Figure 6(a) displays the parameter space derived from the GOA simulation. In this study, the search space was established based on predetermined criteria. Specifically, the population size of grasshoppers was fixed at 20, and the maximum number of iterations was defined as 100. The grasshoppers investigated the several regions inside the search space encompassing the global optimum [18].

The results of this study suggest that the GOA algorithm demonstrates a proficient ability to both explore and exploit in a well-balanced manner, efficiently guiding grasshoppers towards the global optimum. Figure 6(b) depicts the simulation's search history.

This paper elucidates the historical distribution patterns of grasshoppers, focusing on their optimization and search strategies for identifying and establishing more favourable habitats within the available search space. In Figure 6(b), a substantial accumulation of particles is observed at a specific location, indicating the presence of an optimal target within the defined range of parameters.

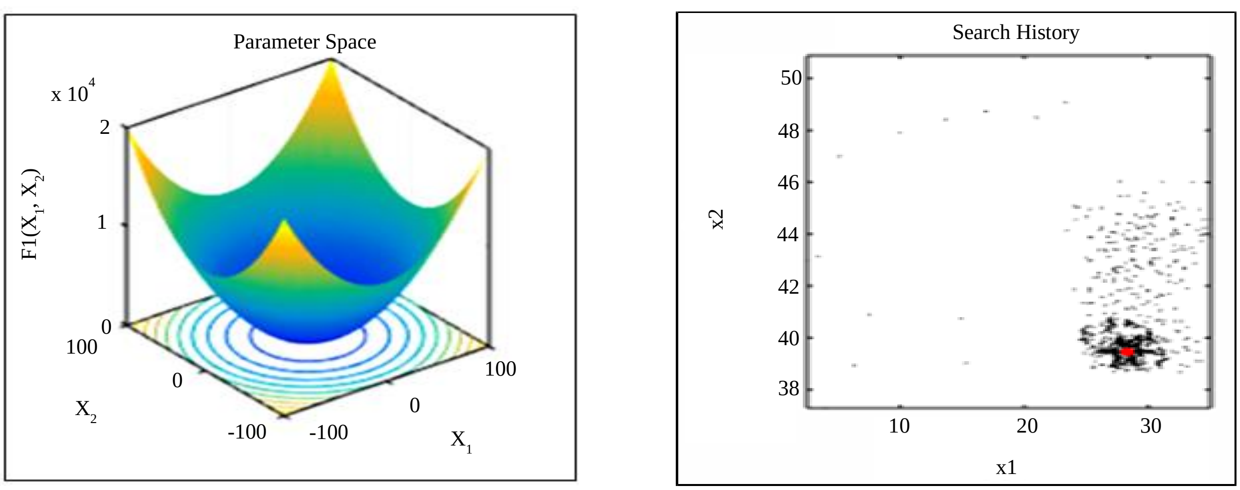

(a) (b)

Fig. 6 Behavior of GOA during optimization (a) Parameter space of GOA, and (b) Search history of GOA.

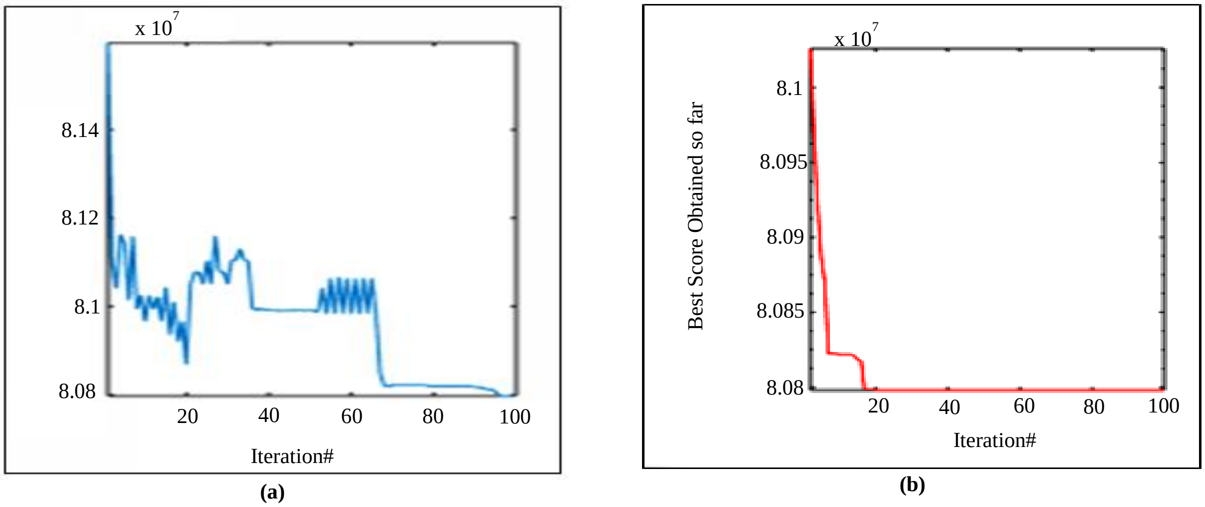

Fig. 7 Fitness behaviour of GOA (a) Average fitness of GOA, and (b) Convergence curve of GOA.

Figure 7 depicts the fitness behavior of the GOA for the entirety of the simulation. Figure 7(a) displays the mean fitness values of all grasshoppers across each iteration. The trajectory curve demonstrates that the grasshoppers underwent substantial adaptations during the initial optimization phases. The occurrence of exploring the search space was prompted by the elevated repulsive rate exhibited by GOA. It is evident that as the optimal conditions are reached, there is a gradual decrease in fluctuation. This phenomenon can be attributed to an adaptive comfort zone and the impact of attractive forces on the grasshoppers [14, 16].

The utilization of the recommended GOA algorithm guarantees the comprehensive exploration and exploitation of the search space, ultimately resulting in convergence at a specific location. This convergence serves as evidence that such behaviour leads to enhanced grasshopper fitness. In the interim, the curve has a downward trend, indicating an improvement in the random population's performance regarding the test functions. Consequently, the accuracy of the estimated optimum over the test functions has also increased. Figure 7(b) illustrates the convergence characteristics of the GOA method, explicitly showcasing the relationship between the number of iterations performed and the corresponding top score achieved. Despite the algorithm being set to execute a maximum of 100 iterations, the optimal score value exhibits a slow convergence towards the minimum, occurring shortly before the 20th iteration.

4. Conclusion

This study has demonstrated the utilization of the Grasshopper Optimization Algorithm (GOA) to identify the ideal sites for Fast Charging Stations (FCS) in a power distribution system. A selection of six FCSs was intentionally made to reduce the overall cost. During the optimization procedure, multiple constraints were considered, encompassing the power distribution system's charging station capacity, load factor, power factor, charging radius, traffic limitations, and security constraints. The methodology employed in this research was assessed by utilizing an IEEE 69-bus distribution test system. The optimization of Electric Vehicle (EV) mobility has been recognized as a crucial factor, assuming that EVs would be moving between a predetermined energy consumption location and an EV charging station that is integrated into the power distribution grid.

The results suggest that the GOA methodology effectively identifies the most suitable sites for Electric Vehicle (EV) charging stations compared to an alternative method.

Funding Statement

This research is supported by the Research Management Institute (RMI), Universiti Teknologi MARA Malaysia, under the Special Research Grant Scheme (600-RMC/GPK5/3 (028/2020)).

References

[1] C. Aravena, and E. Denny, "The Impact of Learning and Short-Term Experience on Preferences for Electric Vehicles," *Renewable and Sustainable Energy Reviews*, vol. 152, pp. 1-9, 2021. [CrossRef] [Google Scholar] [Publisher Link]

[2] Fareed Ahmad et al., "Optimal Location of Electric Vehicle Charging Station and its Impact on Distribution Network: A Review," *Energy Reports*, vol. 8, no. 11, pp. 2314-2333, 2022. [CrossRef] [Google Scholar] [Publisher Link]

[3] Terapong Boonraksa, and Boonruang Marungsri, “Optimal Fast Charging Station Location for Public Electric Transportation in Smart Power Distribution Network,” *2018 International Electrical Engineering Congress (IEECON)*, pp. 1-4, 2018. [CrossRef] [Google Scholar] [Publisher Link]

[4] Hassan S. Hayajneh et al., “Optimal Planning of Battery-Powered Electric Vehicle Charging Station Networks,” *2019 IEEE Green Technologies Conference (GreenTech)*, pp. 1-4, 2019. [CrossRef] [Google Scholar] [Publisher Link]

[5] Nattapong Boonrach, Natin Janjamraj, and Krischonme Bhumkittipich, “Optimal Energy Storage in Residential Micro-Grid for EV Charging Penetration,” *2021 International Conference on Power, Energy and Innovations (ICPEI)*, pp. 37-40, 2018. [CrossRef] [Google Scholar] [Publisher Link]

[6] Krystyna Gomółka, and Piotr Kasprzak, “Directions and Prospects for the Development of the Electric Car Market in Selected ASEAN Countries,” *Energies*, vol. 14, no. 22, pp. 1-16, 2021. [CrossRef] [Google Scholar] [Publisher Link]

[7] M. Etezadi-Amoli, Kent Choma, and Jason Stefani, “Rapid-Charge Electric Vehicle Stations,” *IEEE Transactions on Power Delivery*, vol. 25, no. 3, pp. 1883–1887, 2010. [CrossRef] [Google Scholar] [Publisher Link]

[8] Imtiaz Mahmud Nafi et al., “Effect of Electric Vehicle Fast Charging Station on Residential Distribution Network in Bangladesh,” *2021 5th International Conference on Electrical Engineering and Information Communication Technology (ICEEICT)*, pp. 1-5, 2021. [CrossRef] [Google Scholar] [Publisher Link]

[9] Oscar van Vliet et al., “Energy Use, Cost and CO_2 Emissions of Electric Cars,” *Journal of Power Sources*, vol. 196, no. 4, pp. 2298-2310, 2011. [CrossRef] [Google Scholar] [Publisher Link]

[10] Bálint Csonka, and Csaba Csiszár, “Determination of Charging Infrastructure Location for Electric Vehicles for Electric Vehicle,” *Transportation Research Procedia*, vol. 27, pp. 768-775, 2017. [CrossRef] [Google Scholar] [Publisher Link]

[11] N.H. Kutkut et al., “Design Considerations for Charge Equalization of an Electric Vehicle Battery System,” *IEEE Transactions on Industry Applications*, vol. 35, no. 1, pp. 28–35, 1999. [CrossRef] [Google Scholar] [Publisher Link]

[12] E.M. Valeriote, T.G. Chang, and D.M. Jochim, “Fast Charging of Lead-Acid Batteries,” *Proceedings of 9th Annual Battery Conference on Applications and Advances*, pp. 33–38, 1994. [CrossRef] [Google Scholar] [Publisher Link]

[13] Kazi N. Hasan et al., “Measurement-Based Electric Vehicle Load Profile and Its Impact on Power System Operation,” *2019 9th International Conference on Power and Energy Systems (ICPES)*, pp. 1-6, 2019. [CrossRef] [Google Scholar] [Publisher Link]

[14] Gowthamraj Rajendran et al., “Energy-Efficient Converters for Electric Vehicle Charging Stations,” *SN Applied Sciences*, vol. 2, no. 4, 2020. [CrossRef] [Google Scholar] [Publisher Link]

[15] Mauricio Restrepo, Claudio A. Cañizares, and Mehrdad Kazeran, “Three-Stage Distribution Feeder Control Considering Four-Quadrant EV Chargers,” *IEEE Transactions on Smart Grid*, vol. 9, no. 4, pp. 3736-3747, 2018. [CrossRef] [Google Scholar] [Publisher Link]

[16] Marjan Gjelaj et al., “Optimal Design of DC Fast-Charging Stations for EVs in Low Voltage Grids,” *2017 IEEE Transportation Electrification Conference and Expo (ITEC)*, Chicago, IL, USA, 2017, pp. 684-689. [CrossRef] [Google Scholar] [Publisher Link]

[17] Nopbhorn Leeprechanon, Prakornchai Phonrattanasak, and Mahesh Kumar Sharma, “Optimal Planning of Public Fast Charging Station on Residential Power Distribution System,” *2016 IEEE Transportation Electrification Conference and Expo, Asia-Pacific (ITEC Asia-Pacific)*, Busan, Korea (South), pp. 519-524, 2016. [CrossRef] [Google Scholar] [Publisher Link]

[18] Zi-fa Liu et al., “Optimal Planning of Charging Station for Electric Vehicle Based on Particle Swarm Optimization,” *IEEE PES Innovative Smart Grid Technologies*, Tianjin, China, pp. 1-5, 2012. [CrossRef] [Google Scholar] [Publisher Link]

[19] Payam Sadeghi-Barzani, Abbas Rajabi-Ghahnavieh, and Hosein Kazemi-Karegar, “Optimal Fast Charging Station Placing and Sizing,” *Applied Energy*, vol. 125, pp. 289–299, 2014. [CrossRef] [Google Scholar] [Publisher Link]

[20] Shahrzad Saremi, Seyedali Mirjalili, and Andrew Lewis, “Grasshopper Optimisation Algorithm: Theory and Application,” *Advances in Engineering Software*, vol. 105, pp. 30–47, 2017. [CrossRef] [Google Scholar] [Publisher Link]

[21] Mojtaba Ahanch, Mehran Sanjabi Asasi, and Mojtaba Sedghi Amiri, “A Grasshopper Optimization Algorithm to Solve Optimal Distribution System Reconfiguration and Distributed Generation Placement Problem,” *2017 IEEE 4th International Conference on Knowledge-Based Engineering and Innovation (KBEI)*, Tehran, Iran, pp. 659-0666, 2017. [CrossRef] [Google Scholar] [Publisher Link]

[22] Abhishek G. Neve, Ganesh M. Kakandikar, and Omkar Kulkarni, “Application of Grasshopper Optimization Algorithm for Constrained and Unconstrained Test Functions,” *International Journal of Swarm Intelligence and Evolutionary Computation*, vol. 6, no. 3, 2017. [CrossRef] [Google Scholar] [Publisher Link]

[23] Fareed Danial Ahmad Kahar et al., “Index-Based Transmission for Distributed Generation in Voltage Stability and Loss Control Incorporating Optimization Technique,” *IAES International Journal of Artificial Intelligence (IJ-AI)*, vol. 9, no. 2, pp. 244-251, 2020. [CrossRef] [Google Scholar] [Publisher Link]

[24] Yehia Gad et al., “Smart Energy Management System of Environmentally Friendly Microgrid Based on Grasshopper Optimization Technique,” *Energies*, vol. 13, no. 19, pp. 1-22, 2020. [CrossRef] [Google Scholar] [Publisher Link]